The Journal of Neuroscience, August 1992, 12(8): 2982–2992

Early Appearance of and Neuronal Contribution to Agrin-like Molecules at Embryonic Frog Nerve–Muscle Synapses Formed in Culture

M. W. Cohen[1] and E. W. Godfrey[2]

[1]Department of Physiology, McGill University, Montreal, Quebec, Canada H3G 1Y6 and [2]Department of Cellular Biology and Anatomy, Medical College of Wisconsin, Milwaukee, Wisconsin 53226

Antibodies against chicken and *Torpedo* agrin were used for immunofluorescent staining in order to assess the spatial distribution and temporal appearance of agrin-like molecules at newly formed synaptic contacts in cultures of embryonic *Xenopus* nerve and muscle cells. The antibodies stained *Xenopus* neuromuscular junctions and removed ACh receptor (AChR)-aggregating activity from extracts of *Xenopus* brain. Immunofluorescence was observed at almost all nerve-induced AChR aggregates, even at microaggregates in cocultures as young as 7.5 hr and at nerve–muscle contacts less than 2 hr old. Microdeposits of immunofluorescence extended as far distally as, or farther than, the microaggregates of AChRs along young nerve–muscle contacts. They also occurred along portions of growing neurites that were not in contact with muscle. By contrast, immunofluorescence was rarely observed at the nonsynaptic aggregates of AChRs that form on noninnervated muscle cells. These results raise the possibility that neuronally derived microaggregates of agrin-like molecules may be primary sites of nerve-induced clustering of AChRs, and they indicate that these molecules are present at embryonic nerve–muscle synapses from the very onset of AChR aggregation.

The cellular origin of the agrin-like molecules at synapses was examined in cross-species cocultures in which the neurons and muscle cells were obtained from embryos of *Xenopus laevis* and *Rana pipiens*. Immunofluorescent staining with anti-agrin antibodies reactive at both *Rana* and *Xenopus* neuromuscular junctions revealed immunofluorescence at AChR aggregates along nerve–muscle contacts involving both cross-species combinations. Immunofluorescent staining with an anti-agrin antibody reactive at *Rana* but not at *Xenopus* neuromuscular junctions was positive only at cross-species nerve–muscle contacts involving *Rana* neurons. These results provide the first demonstration that embryonic neurons supply agrin-like molecules to the synapses they form with embryonic muscle cells.

Received Oct. 25, 1991; revised Feb. 7, 1992; accepted Mar. 10, 1992.

This work was supported by MRC of Canada Grant MT3630 to M.W.C. and NIH Grants NS27218 and HD20743 to E.W.G. We thank D. McDonald, P. Vardaxis, G. Hébert, N. Drzewiecki, and K. Gradall for photographic and technical assistance.

Correspondence should be addressed to M. W. Cohen, Department of Physiology, McGill University, 3655 Drummond, Montreal, Quebec, Canada H3G 1Y6.

A cardinal event in neuromuscular synaptogenesis is the aggregation of ACh receptors (AChRs) in the newly forming postsynaptic membrane. This aggregation is nerve induced, and it begins within a few hours at sites where growing axons contact embryonic muscle cells (Anderson et al., 1977; Cohen et al., 1979; Frank and Fischbach, 1979; Chow and Cohen, 1983). Current evidence indicates that agrin, or a closely related molecule, is the neuronal agent that triggers this aggregation of AChRs at the developing neuromuscular junction (McMahan and Wallace, 1989; Wallace, 1991). Agrin-like molecules are present in the synaptic cleft of the mature neuromuscular junction (Fallon et al., 1985; Reist et al., 1987) and at almost all AChR aggregates in embryonic muscle (Godfrey et al., 1988b; Fallon and Gelfman, 1989). These molecules are also present in motor neurons and are transported anterogradely along the axons (Magill-Solc and McMahan, 1988, 1989). Furthermore, agrin causes clustering of AChRs on embryonic muscle cells in culture in the absence of nerve cells (Godfrey et al., 1984; Nitkin et al., 1987), and agents that inhibit this activity of agrin also inhibit nerve-induced aggregation of AChRs (Hirano and Kidokoro, 1989; Wallace, 1990).

Although these findings are consistent with the hypothesis that agrin is the neuronal agent that triggers AChR aggregation during neuromuscular synaptogenesis, other results tend to complicate this issue. Agrin-like molecules are expressed not only in motor neurons but also in a variety of other cell types including muscle (Reist et al., 1987; Godfrey et al., 1988a,b; Godfrey, 1991; Rupp et al., 1991). They have also been observed at AChR aggregates that develop on noninnervated muscle cells in aneural limbs of chick embryos (Fallon and Gelfman, 1989). Such findings suggest that agrin-like molecules at developing neuromuscular junctions may be derived from muscle cells as well as neurons. In fact, these molecules appear in the limb bud mesenchyme of the chick embryo prior to muscle differentiation or ingrowth of motor axons (Godfrey et al., 1988b; Fallon and Gelfman, 1989). Accordingly, it is unclear whether neuronally derived agrin-like molecules are present at embryonic neuromuscular junctions from the onset of nerve-induced aggregation of AChRs.

We have addressed this question in cocultures of embryonic frog nerve and muscle cells. Two types of AChR aggregates can be readily distinguished on the muscle cells in these cultures: those that are nerve induced and associated with synaptogenesis, and those that develop in the absence of innervation (Anderson and Cohen, 1977; Anderson et al., 1977; Kidokoro et al., 1980). Our findings, based on immunofluorescence with anti-agrin an-

tibodies, indicate that the agrin-like molecules investigated in this study are present on growing neurites and at the earliest-detectable, nerve-induced microaggregates of AChRs but not at nonsynaptic aggregates of AChRs. Additional experiments, in which cross-species (*Xenopus laevis* and *Rana pipiens*) cocultures were stained with anti-agrin antibodies having different species specificities, confirm that embryonic neurons do indeed supply agrin-like molecules to the synapses they form on embryonic muscle cells.

A brief report of some of this work has appeared in abstract form (Cohen and Godfrey, 1991).

Materials and Methods

Cultures. The method of preparing cultures from embryos of *Xenopus laevis* was similar to that of Cohen et al. (1987). Myotomal muscle cells, derived from 1-d-old embryos, were plated in glass culture chambers (Anderson et al., 1977). In most cases, the substrate was rat tail collagen (Bornstein, 1958) and mouse laminin (kindly provided by S. Carbonetto of McGill University); otherwise, it was only collagen. Laminin enhanced neuritic growth but had no other apparent effect on the results reported here. Freshly dissociated spinal cord cells were added to most of the cultures 1–2 d after plating the muscle cells. The remaining cultures were retained as pure muscle cultures.

For some cultures we used *Rana pipiens* embryos, which were kindly provided by P. Pasceri of R. Elinson's laboratory at the University of Toronto. Myotomal muscle and spinal cords were obtained from embryos 3.3–4.8 mm in length, equivalent to stages 17–19 of Shumway (1940). The techniques for isolating and dissociating these tissues from *Rana* embryos, as well as the culture conditions, were similar to those for *Xenopus* nerve–muscle cultures.

In cocultures involving *Rana* nerve and/or muscle cells, as in pure *Xenopus* cocultures, some spontaneous twitching was observed among nerve-contacted muscle cells. Such twitching reflects functional innervation and never occurs among the noninnervated muscle cells in these amphibian cultures (Cohen, 1972; Anderson et al., 1977; Kidokoro et al., 1980; Swenarchuk et al., 1990). It was prevented in the present study by including 0.2 μg/ml tetramethylrhodamine-conjugated α-bungarotoxin (RαBT; Molecular Probes) in the culture medium. In freshly dissected myotomal muscles from tadpoles, postlabeling with ^{125}IαBT (see Goldfarb et al., 1990) indicated that 2 μg/ml RαBT labeled all AChRs within 1 hr, and at 0.2 μg/ml more than 70% were labeled in 3 hr.

Cultures were maintained at room temperature (23–25°C). In most cases they were processed (see below) within 2 d of plating the spinal cord cells, but in a few initial experiments some cocultures were as old as 4 d.

Antibodies. Anti-agrin antibodies were prepared and characterized previously. Rabbit antiserum 36 (anti-36) was prepared against a 72 kDa affinity-purified agrin-like protein derived from extracellular matrix of chicken kidney (Godfrey, 1991). Preimmune serum (pre-36) from the same rabbit served as a control. Monoclonal antibodies C3 and F11 (in mouse ascites fluid) were prepared against affinity-purified agrin derived from extracellular matrix of *Torpedo* electric organ, and are also reactive with chick agrin (Godfrey et al., 1988b). Monoclonal antibody 5B1, also prepared against *Torpedo* agrin, was a generous gift from R. M. Nitkin (NIH, Bethesda, MD). It labels neuromuscular junctions in chick and *Rana pipiens* (Reist et al., 1987). In addition, we used a rabbit antiserum against laminin (GIBCO).

Affintiy-purified, fluorescein-conjugated goat immunoglobulins (Organon Teknika-Cappel, Molecular Probes) were used as secondary antibodies to visualize the binding sites of the primary antibodies. They were anti-rabbit for the antisera and preimmune serum and anti-mouse for the monoclonal antibodies.

Immunoprecipitation of AChR-aggregating activity. Binding of antibodies to AChR-aggregating molecules was assessed by measuring the ability of immobilized antibodies to remove activity from a supernatant fraction (31,000 × *g*, 20 min) of adult *Xenopus* brain homogenates. Immunoprecipitation was carried out by binding antibodies to protein A–Sepharose beads, either directly (for rabbit sera) or indirectly (for monoclonals) through goat anti-mouse IgG, as previously described (Godfrey, 1991). For each anti-agrin antibody tested, 15 μl of protein A–Sepharose beads, and either 45 μl of rabbit serum or 100 μg of affinity-purified goat anti-mouse IgG (Cappel) followed by 300 μl of ascites fluid (monoclonal antibody), was used to precipitate activity from brain homogenate containing ~5 units of AChR-aggregating activity (Godfrey et al., 1984). The supernatant was then assayed in triplicate for AChR-aggregating activity using chick embryo skeletal myotube cultures (~1.5 units/culture).

Fluorescent staining of cultures. Prior to incubation in primary antibody, cultures were bathed in a solution of 67% (v/v) L15 and 1% (v/v) goat serum (L15-GS) for at least 20 min at ~6°C. The remainder of the staining protocol was carried out at the same low temperature. L15-GS was used for all dilutions and rinses. Anti-36 and pre-36 (1:1000), monoclonal antibodies (1:200), and secondary antibodies (1:100) were filtered (Millex GV, Millipore; pore size, 0.22 μm) before use. Incubation times were 1 hr. After each antibody, cultures were rinsed seven times over a period of 40–60 min.

Stained cultures were fixed as described previously (Cohen et al., 1987) and stored in fixative at ~6°C for 2–5 d. They were subsequently rinsed, cleared with 90% (v/v) glycerol containing 1 mg/ml *p*-phenylenediamine and 10 mM sodium carbonate, and stored at −16°C.

When fluorescent staining was carried out within 12 hr of plating the spinal cord cells, the primary antibody solution also contained 2–4 μg/ml RαBT to ensure that all AChRs would be stained. In some cases, fields of growing neurites were photographed in young cocultures before beginning the staining protocol so that the age of newly formed neurite–muscle contacts could be known more precisely. In estimating these ages, we have assumed that neuritic growth and aggregation of AChRs ceased within 30 min of beginning the incubation in primary antibody. By that time, the culture had been at ~6°C for at least 50 min (see above). At this temperature *Xenopus* embryos cease to develop, and at 14°C their rate of development is about one-third of that at 23–25°C. Thus, our age estimates are probably accurate within ±0.5 hr.

Microscopy and analysis. Incident-light fluorescence optics and transmitted-light phase-contrast optics were used separately and in combination so that the cellular location of sites of fluorescence could be properly assessed. Each patch of RαBT fluorescence at least 2 μm in length and separated from its neighbors by 2 μm or more was considered a single aggregate of AChRs. Colocalization of immunofluorescence at these RαBT patches was readily evaluated directly through the microscope. To analyze colocalization of immunofluorescence at micropatches of RαBT fluorescence (< 1 μm diameter), we used photographs taken through an oil immersion objective (100×, NA 1.3) and enlarged to 1.4 mm/μm. The positions of RαBT micropatches were marked on a transparency that was placed on the corresponding photograph of immunofluorescence. Colocalization was defined as overlap of the RαBT micropatch and immunofluorescence.

Although RαBT (MW, ~8000) readily stains synaptic and nonsynaptic aggregates of AChRs on the lower surface of the muscle cells, antibodies appeared to have much poorer access to this surface. For example, anti-36 immunofluorescence was almost always present at synaptic AChR aggregates on the edge or upper surface of the muscle cells, whereas the incidence of colocalization and the intensity of the immunofluorescence were less at synaptic aggregates on the lower surface. An even greater difference was observed when we stained with anti-laminin. Anti-laminin immunofluorescence was present at virtually all "exposed" nonsynaptic AChR aggregates but was rarely observed at "lower surface" ones. Restricted access of antibodies, compared to RαBT, was also apparent after staining freshly dissected muscles (see below). Accordingly, in assessing whether or not anti-agrin immunofluorescence was present at sites of RαBT fluorescence in cultures, all lower surface sites were excluded. However, some photographic examples of colocalization on the lower surface have been included because the nerve–muscle contacts remain in the same plane of focus.

Fluorescent staining of muscles. To examine the reactivity of anti-agrin antibodies at frog neuromuscular junctions formed *in vivo,* the following muscles were used: myotomal muscles from stage 46–49 *Xenopus* tadpoles (see Nieuwkoop and Faber, 1967), from stage 26–30 *Xenopus* embryos, and from *Rana* tadpoles 11–13 mm in length, as well as sartorius muscles from *Rana* frogs weighing 4–7 gm. Although the former muscles are relatively small and all their neuromuscular junctions are stained brightly after 1 hr in 2 μg/ml RαBT, the staining protocol described above revealed immunofluorescence only at neuromuscular junctions near the surface. To enhance penetration of antibodies, primary antibody was applied for 5–16 hr (anti-36 and pre-36 at 1:5000, monoclonal antibodies at 1:1000) and secondary antibody (1:100) for 3–5 hr. Otherwise, the staining protocol was the same as that described for the cultures. Penetration of antibodies was less com-

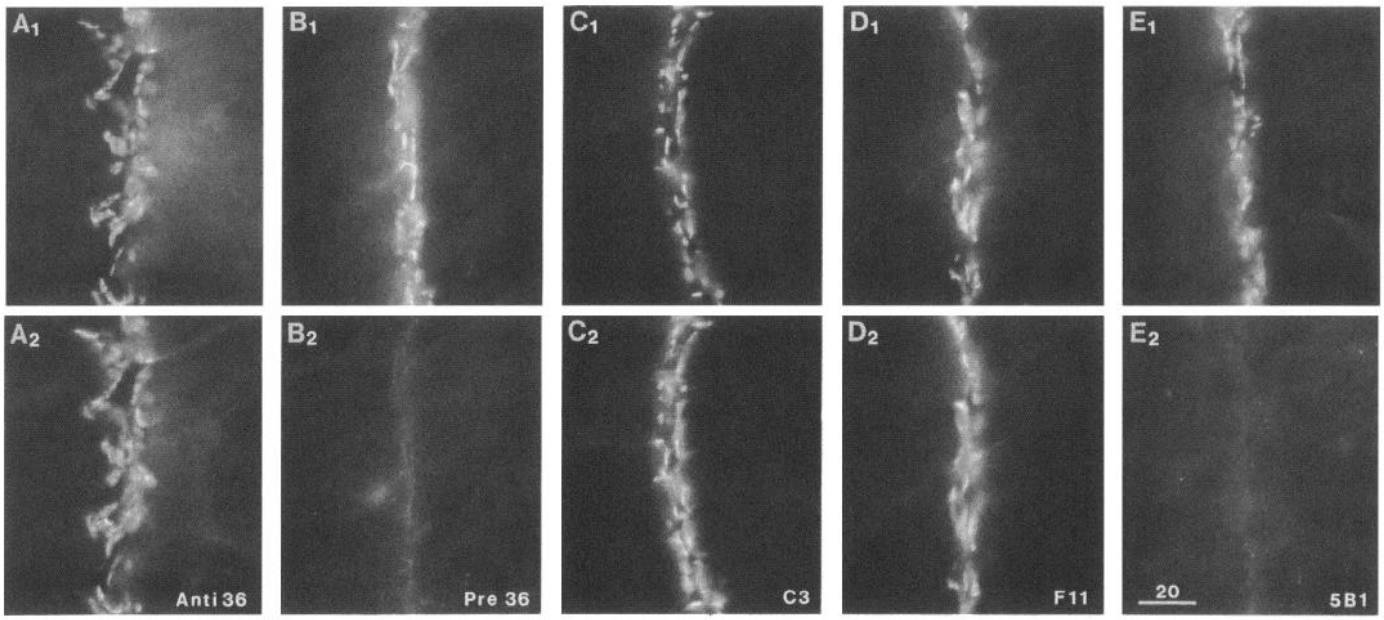

Figure 1. Anti-agrin immunofluorescence at synapses in myotomal muscle of *Xenopus* tadpoles. RαBT fluorescence is seen in A_1–E_1. The corresponding immunofluorescence is seen in the lower micrographs: anti-36 in A_2, pre-36 in B_2, C3 in C_2, F11 in D_2, and 5B1 in E_2. Anti-36, C3, and F11 stained synaptic sites, whereas pre-36 and 5B1 did not. Scale bar, 20 μm.

plete in *Rana* tadpole myotomes than in *Xenopus* tadpole myotomes, and poorer removal of unbound antibody in the former may account for some diffuse, nonspecific fluorescence along the intermyotomal junctions (see Fig. 7). After staining and fixing, right and left myotomes were separated from each other and from spinal cord and notochord, cleared as described above, and mounted on glass slides. In the case of the sartorius muscle, small bundles of fibers were teased from the surface and then mounted.

Interestingly, the barriers to penetration of antibodies were most severe in myotomal muscles from *Xenopus* embryos. Although synapses in these muscles were readily stained with RαBT, they were rarely revealed even by overnight immunofluorescent staining. To provide better accessibility to the medial surface, where synapses first form, the right and left myotomes were separated from each other and from spinal cord and notochord after mild prefixation. The staining protocol described for cultures was then applied with success, using incubation times of 1 hr for both primary and secondary antibodies.

Results

Anti-agrin immunofluorescence in Xenopus *muscles*

In order to evaluate the usefulness of antibodies raised against chicken and *Torpedo* agrin for immunofluorescent staining of *Xenopus* nerve–muscle cocultures, their staining patterns were first examined in the myotomal muscle of *Xenopus* tadpoles. Figure 1 illustrates synaptic aggregates of AChRs in this muscle (A_1–E_1) and the corresponding immunofluorescence (A_2–E_2). Synaptic sites were stained brightly with anti-36 (Fig. 1*A*) but were not stained with pre-36 (Fig. 1*B*). Monoclonal antibodies C3 and F11 stained synaptic sites almost as brightly as anti-36 (Fig. 1*C,D*), whereas there was no detectable staining of synaptic sites with 5B1 (Fig. 1*E*). Interestingly, 5B1 is reactive at neuromuscular junctions in muscles of *Rana pipiens* (Reist et al., 1987; see also below).

Specific immunofluorescence (observed with anti-36, C3 or F11 but not with pre-36 or 5B1) was also seen at the caudalmost (youngest) microaggregates of AChRs in myotomal muscle from *Xenopus* embryos (Fig. 2). Portions of the thin sheath (dermatome) on the lateral surface of the myotomes in embryos and tadpoles, and remnants of tissue remaining on the medial surface of embryonic myotomes after removal of the notochord and spinal cord (see Materials and Methods), also exhibited specific immunofluorescence (not shown).

Immunoprecipitation of AChR-aggregating activity from Xenopus *brain*

The ability of the anti-agrin antibodies to remove AChR-aggregating activity from adult *Xenopus* brain homogenate was

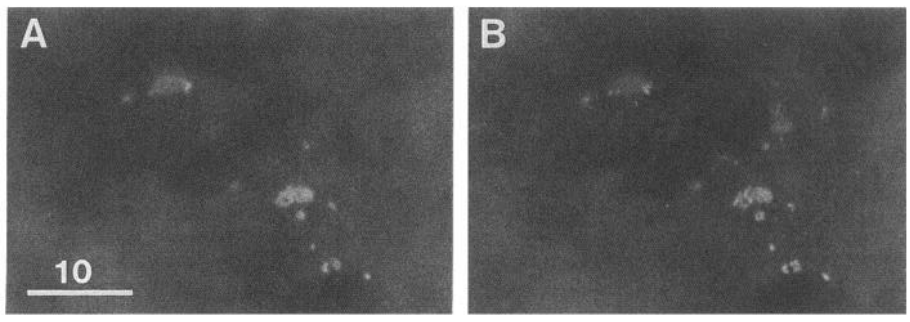

Figure 2. Colocalization of anti-36 immunofluorescence at AChR aggregates in myotomal muscle of a 1-d-old (stage 27) *Xenopus* embryo. *A*, RαBT fluorescence along the medial surface of the most caudally occurring (youngest) myotome that had detectable AChR aggregates. *B*, Immunofluorescence is present at all sites of AChR aggregation as well as at a few additional sites. Scale bar, 10 μm.

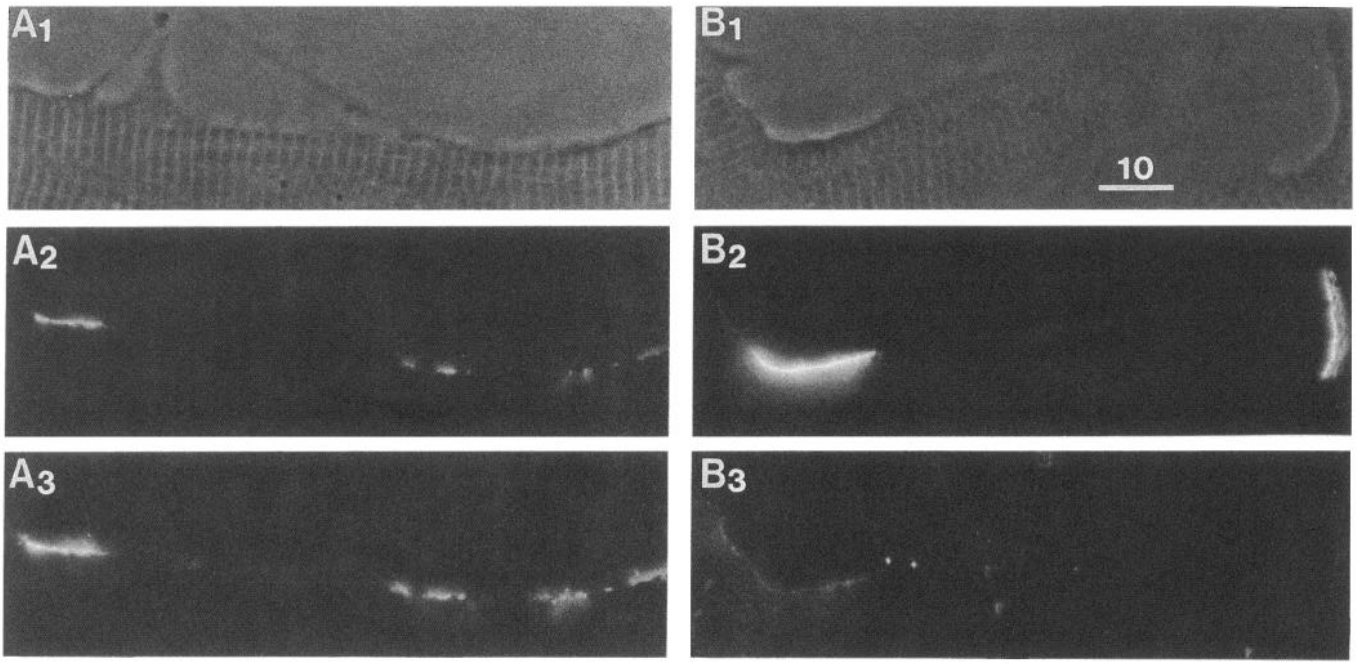

Figure 3. Anti-36 immunofluorescence at synaptic, but not at nonsynaptic, aggregates of AChRs. Phase contrast (A_1, B_1), RαBT fluorescence (A_2, B_2), and immunofluorescence (A_3, B_3) are shown. Bright immunofluorescence (A_3) was colocalized with the RαBT fluorescence (A_2) along the nerve–muscle contact (A_1) but was not apparent at nonsynaptic AChR aggregates (B_1–B_3). The faint immunofluorescence seen in B_3 was also obtained with pre-36 and 5B1, and is considered to be nonspecific. Bright speckles of immunofluorescence (B_3) occurred randomly throughout the culture, even on bare portions of the culture dish, and are also considered to be nonspecific since they were seen with all primary antibodies, including pre-36 and 5B1. The nonsynaptic AChR aggregates extend above and below the plane of focus. Scale bar, 10 μm.

measured using a previously developed immunoprecipitation assay. Anti-36, C3, and F11 removed 77–91% of the AChR-aggregating activity, whereas pre-36 and 5B1 precipitated only 7–18% of the activity (Table 1). Thus, the antibodies that stained *Xenopus* neuromuscular junctions were reactive with AChR-aggregating molecules—probably agrin—from *Xenopus* brain. The possibility that they also reacted with "inactive" agrin-like proteins (Godfrey, 1991; Ruegg et al., 1991) is considered in the Discussion.

Anti-agrin immunofluorescence in Xenopus *cultures*

In nerve–muscle cultures, as in normal muscles, there was extensive colocalization between synaptic aggregates of AChRs and anti-agrin immunofluorescence. Figure 3*A* shows an example with anti-36 staining. Immunofluorescence is seen associated with the full length of all synaptic AChR aggregates along the nerve–muscle contacts. By contrast, nonsynaptic aggregates of AChRs on noninnervated muscle cells exhibited little if any immunofluorescence. This was the case in pure muscle cultures as well as in nerve–muscle cocultures. In the example shown in Figure 3*B*, there was essentially no detectable anti-36 immunofluorescence at one of the nonsynaptic AChR aggregates, and at the second one the immunofluorescence was very faint and extended beyond the limits of the bright RαBT fluorescence. On the other hand, the nonsynaptic sites of AChR aggregation did stain brightly for laminin (not shown).

The results for all experiments are summarized in Figure 4. The incidence of colocalization of immunofluorescence at synaptic AChR aggregates was 96% for anti-36, 88% for C3, and 91% for F11 compared to 0% for pre-36 and 5B1. These results were independent of the age of the coculture. By contrast, immunofluorescence at nonsynaptic AChR aggregates amounted to only 5% for anti-36, 2% for pre-36, and 1% for F11. These few positive examples were relatively faint (as in Fig. 3*B*) and likely represent nonspecific binding of antibodies. Altogether, the results indicate that the agrin-like molecules recognized by anti-36, C3, and F11 are present in high concentration at synaptic aggregates of AChRs but are virtually absent at nonsynaptic ones. This situation in *Xenopus* nerve–muscle cultures stands in apparent contrast (but see Discussion) to that in chick embryonic muscle, where high concentrations of agrin-like molecules have been detected at nonsynaptic AChR aggregates (Fallon and Gelfman, 1989).

In addition to the anti-agrin immunofluorescence along nerve–muscle contacts, bright immunofluorescence was occasionally seen in association with a subpopulation of flat transparent non-muscle cells (not shown). In individual cultures, the number of

Table 1. Immunoprecipitation of AChR-aggregating activity from *Xenopus* brain

Antibody	Activity precipitated (%)	
	Exp 1	Exp 2
Anti-36	85	86
Pre-36	18	11
C3	87	91
F11	77	80
5B1	9	7

Antibodies were bound to protein A–Sepharose beads and incubated with a supernatant fraction of adult *Xenopus* brain homogenate (protocol in Godfrey, 1991; see Materials and Methods). Beads without antibody were used to define 0% specific precipitation; AChR aggregation in untreated chick muscle cultures was used to define the 100% precipitation level. Data shown represent averages from triplicate AChR aggregation assays.

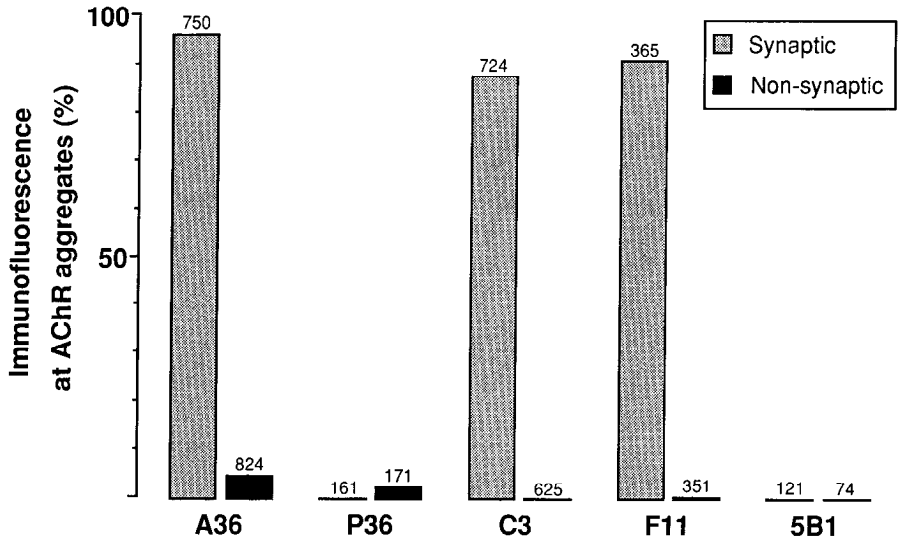

Figure 4. Incidence of colocalization of immunofluorescence at synaptic and nonsynaptic AChR aggregates in culture. For each antibody, the result for synaptic aggregates is plotted on the *left* (*shaded columns*) and the result for nonsynaptic ones is plotted on the *right* (*solid columns*). The *numbers* of AChR aggregates counted are indicated above the columns. There was a high incidence of colocalization only at synaptic aggregates and only with anti-36, C3, and F11.

such examples varied between zero and six. This immunofluorescence appeared to be specific because it was seen in cultures stained with anti-36, C3, and F11 but not in those stained with pre-36 or 5B1. We are uncertain of the identity of these cells, but they may be dermatomal in view of the anti-agrin immunofluorescence associated with the dermatomal surface of *Xenopus* myotomal muscles.

Anti-agrin immunofluorescence at nerve-induced microaggregates of AChRs in 7.5-hr-old Xenopus *cocultures*

The data presented so far are based on AChR aggregates that were at least 2 μm in length (see Materials and Methods). However, in 7.5-hr-old cocultures, most of the synaptic AChR aggregates were less than 1 μm in their greatest dimension and many were even less than 0.5 μm. A total of 640 synaptic microaggregates of AChRs were observed in 34 fields in six cultures, and 541 (84.5%) of them had colocalized anti-agrin immunofluorescence (Figs. 5, 6). The high incidence of colocalization was similar whether we used anti-36, C3, or F11.

In young living cocultures, neurite outgrowth was first seen about 3 hr after plating the neurons. Accordingly, it is likely that almost all nerve–muscle contacts in our 7.5-hr-old cocultures were less than 5 hr old. In some cultures, a number of fields were photographed prior to processing, so that the age of the contacts could be known more precisely. Altogether, 35 synaptic AChR microaggregates were observed at contacts less than 2 hr old and 32 (91.4%) of them had colocalized anti-agrin immunofluroescence (Figs. 5*D*, 6). Colocalization occurred even at barely detectable AChR microaggregates and even when the nerve–muscle contacts were less than 1.5 hr old (Fig. 6).

Further evidence that agrin-like molecules were present at most, if not all, synaptic sites from the onset of their formation is suggested by the following observations. In 24 fields where the most distally occurring AChR microaggregate could be reliably identified, 21 (87.5%) of these "youngest" synaptic sites of AChR aggregation had colocalized immunofluorescence (Figs. 5*E*, 6). In 12 of these fields there were microdeposits of immunofluorescence even more distally along the nerve–muscle contact (Fig. 6). Other portions of young neurite–muscle contacts also exhibited microdeposits of immunofluorescence that were not associated with microaggregates of AChRs, so that often the former outnumbered the latter (Figs. 5*D*, 6). Such "AChR-free" sites of anti-agrin immunofluorescence along nerve–muscle contacts were seen in 31 (91.2%) of 34 fields examined and may represent sites of future AChR aggregation (see Discussion).

In the example of Figure 6, it is apparent that the microdeposits of immunofluorescence were associated not only with the nerve–muscle contact but also with the nonsynaptic side of the neurite. Even portions of neurite that were not in contact with muscle cells exhibited microdeposits of immunofluorescence (Fig. 5*F*). Such examples were observed in 13 (76.5%) of 17 fields where the "contact-free" portions of neurite were at least 50 μm in length. Microdeposits of immunofluorescence on "contact-free" portions of neurites were observed in young cocultures stained with anti-36, C3, or F11 but were rare when the staining was carried out with pre-36 or 5B1. Older cocultures in which neuritic growth is reduced exhibited a much lower incidence of anti-agrin immunofluorescence along their neurites. It may be that agrin molecules bind transiently to the outer surface of growing neurites at, or close to, sites where they are externalized.

The localization of anti-agrin immunofluorescence along

→

Figure 5. F11 immunofluorescence in a 7.5-hr-old coculture. *A*, Phase contrast of living culture. *B*, The same field, 2 hr later (see Materials and Methods), photographed after fixation. During the 2 hr interval between *A* and *B*, the neurite grew and established new contacts with some of the muscle cells. The *boxed areas* in *B* are shown at higher magnification in C_1, D_1, E_1, and F_1, respectively. The corresponding RαBT fluorescence is shown in C_2–F_2, and the immunofluorescence, in C_3–F_3. There was immunofluorescence at all synaptic aggregates of AChRs, including those in *D* and *E* where the nerve–muscle contacts were less than 2 hr old. Note in *D* the presence of immunofluorescence even at barely detectable AChR microaggregates as well as the additional sites of immunofluorescence along the contact. Note in *E* that bright immunofluorescence was associated with the synaptic aggregates of AChRs but not with the large, bright nonsynaptic aggregate. Note in *F* the immunofluorescence along the neurite. Scale bars: *B*, 30 μm for *A* and *B*; E_1, 10 μm for *C*–*F*.

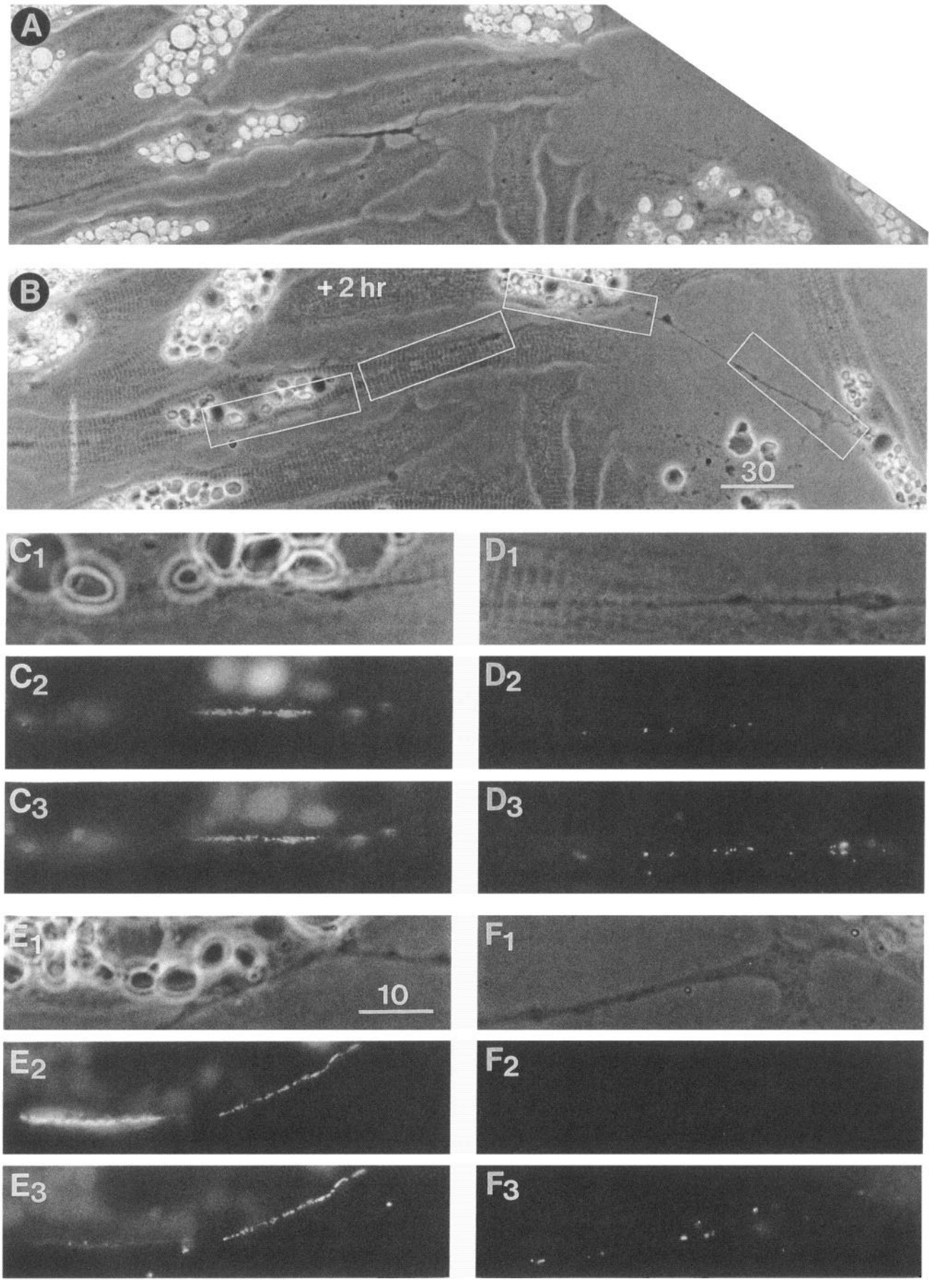
A
B
+2 hr
30
C1
C2
C3
D1
D2
D3
E1
10
E2
E3
F1
F2
F3

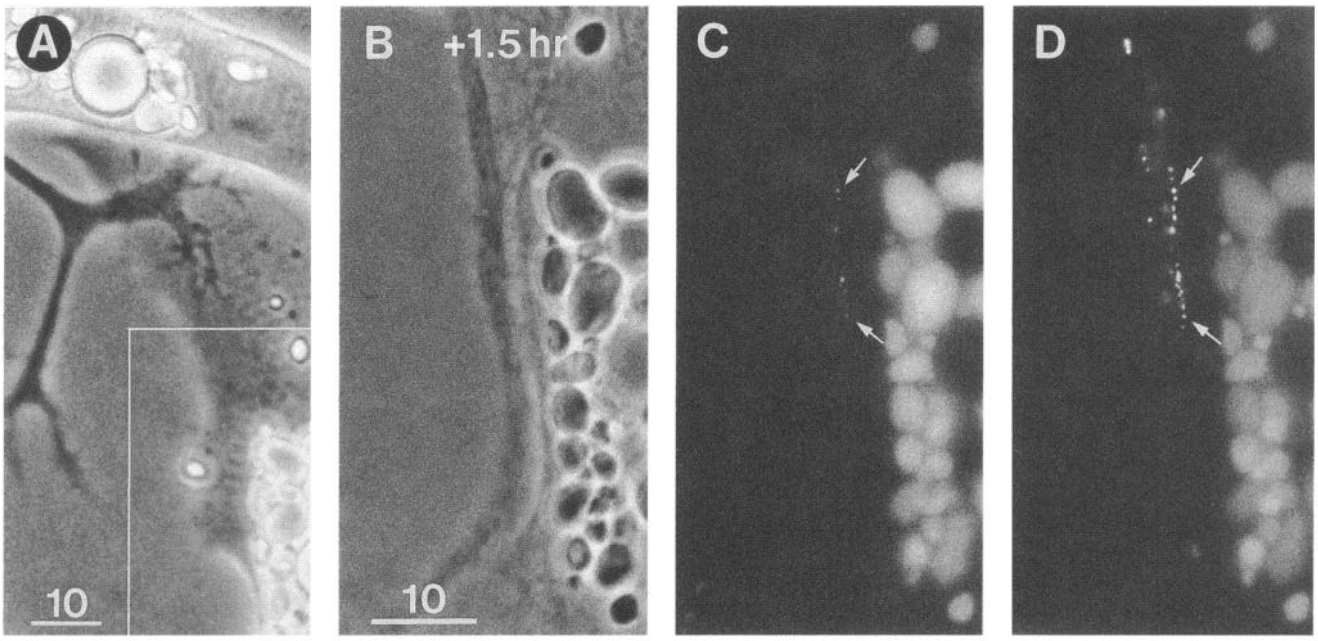

Figure 6. Anti-36 immunofluorescence along a nerve–muscle contact less than 1.5 hr old. *A*, Phase contrast of living culture. The *boxed area* shows a portion of muscle cell that, during the subsequent 1.5 hr, became contacted by the growing neurite. *B*, Higher magnification of the newly established contact, photographed after fixation. *C*, RαBT fluorescence. *Arrows* point to the most proximal and most distal AChR microaggregates along the contact. *D*, Immunofluorescence, with *arrows* pointing to the same sites as in *C*. Note that even the barely detectable AChR aggregates had relatively bright immunofluorescence associated with them, and that there were additional sites of immunofluorescence along the contact as well as on the nonsynaptic side of the neurite. Scale bars: *A*, 10 μm; *B*, 10 μm for *B–D*.

growing neurites and at nerve–muscle synapses but not at nonsynaptic AChR aggregates on muscle cells suggests that the neurons supplied agrin-like molecules to the synapses. As described below, this was investigated more directly in cross-species cocultures derived from *Rana pipiens* and *Xenopus laevis* embryos. As an initial step, we tested the reactivity of the anti-agrin antibodies in *Rana* muscles.

Anti-agrin immunofluorescence in Rana *muscles*

In *Rana* as in *Xenopus* myotomal muscle, anti-36 (Fig. 7*A*), C3, and F11 stained synaptic sites whereas pre-36 (Fig. 7*B*) did not. On the other hand, unlike the case for *Xenopus* myotomal muscle, 5B1 also stained synaptic sites in *Rana* myotomal muscle (Fig. 7*C*). This is in agreement with the finding of Reist et al. (1987) that 5B1 is reactive at *Rana* neuromuscular junctions. Although not evident in Figure 7, the 5B1 immunofluorescence was generally fainter than the immunofluorescence seen with anti-36, C3, and F11.

Similar results were obtained using *Rana* sartorius muscles. Examples for C3 and 5B1 are shown in Figure 8. The immunofluorescence consisted of a series of intense transverse bands separated by intervals of ~1 μm where the immunofluorescence was less intense. This characteristic pattern matched that of the RαBT fluorescence associated with the AChRs. It was also obtained with anti-36 and F11, but not with pre-36, and is consistent with the demonstration by Reist et al. (1987) that anti-agrin binding sites at *Rana* neuromuscular junctions are present along the entire synaptic cleft and extend into the junctional folds. The banded pattern is not seen at the neuromuscular junctions of tadpole myotomal muscle because such neuromuscular junctions lack junctional folds (Kullberg et al., 1977).

Besides its presence at synaptic sites, specific immunofluorescence was also seen in association with the thin sheath (dermatome) covering the lateral surface of the myotomes (not shown). Nonspecific immunofluorescence was observed along portions of intermyotomal junctions in the vicinity of synaptic sites (Fig. 7) and in association with connective tissue in sartorius muscles (Fig. 8).

Anti-agrin immunofluorescence in cross-species cocultures

The four different combinations of nerve–muscle coculture are designated as follows: SC_X-M_X, in which the spinal cord cells (SC) and myotomal muscle cells (M) were derived from *Xenopus* embryos (X); SC_R-M_R, in which the cells were derived from *Rana* embryos (R); SC_R-M_X; and SC_X-M_R.

In SC_R-M_R cultures, the results were in agreement with those obtained with freshly dissected *Rana* muscles. Synaptic aggregates of AChRs (along nerve–muscle contacts) exhibited colocalized immunofluorescence when the staining was done with anti-36, C3, F11, or 5B1. As was the case in SC_X-M_X cultures, there was little if any immunofluorescence elsewhere on the muscle cells, including sites of nonsynaptic AChR aggregates. As shown in Figure 9, the incidence of colocalization at synaptic AChR aggregates along SC_R-M_R contacts was 93% for anti-36, C3, and F11, similar to that seen in SC_X-M_X cultures. The corresponding value for 5B1 was 76%, somewhat lower than for the other antibodies presumably because of the lower intensity of the 5B1 immunofluorescence. In any event 5B1 was, as expected, effective in revealing agrin-like molecules at synaptic AChR aggregates in SC_R-M_R cultures, whereas in SC_X-M_X cultures it was completely ineffective. Therefore, this antibody was used to assess the cellular origin of agrin-like molecules at nerve–muscle contacts in cross-species cultures.

In SC_R-M_X cultures, there was extensive colocalization of 5B1

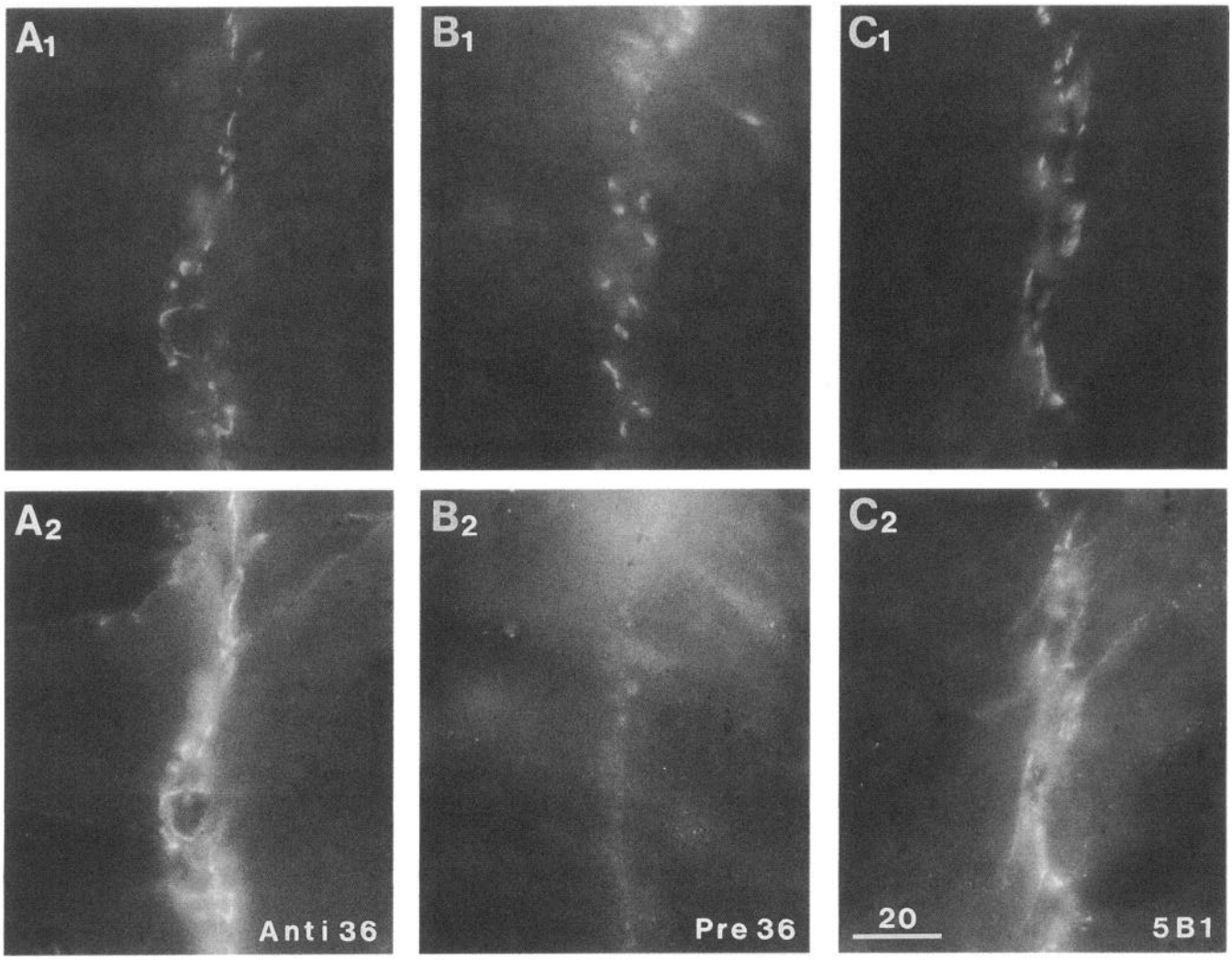

Figure 7. Anti-agrin immunofluorescence at synapses in myotomal muscle of *Rana* tadpoles. RαBT fluorescence is seen in A_1–C_1. The corresponding immunofluorescence is seen in the lower micrographs: anti-36 in A_2, pre-36 in B_2, and 5B1 in C_2. The anti-agrin antibodies, but not the preimmune serum, stained synaptic sites. Some diffuse, nonspecific immunofluorescence is also apparent in the vicinity of some synaptic sites. Scale bar, 20 μm.

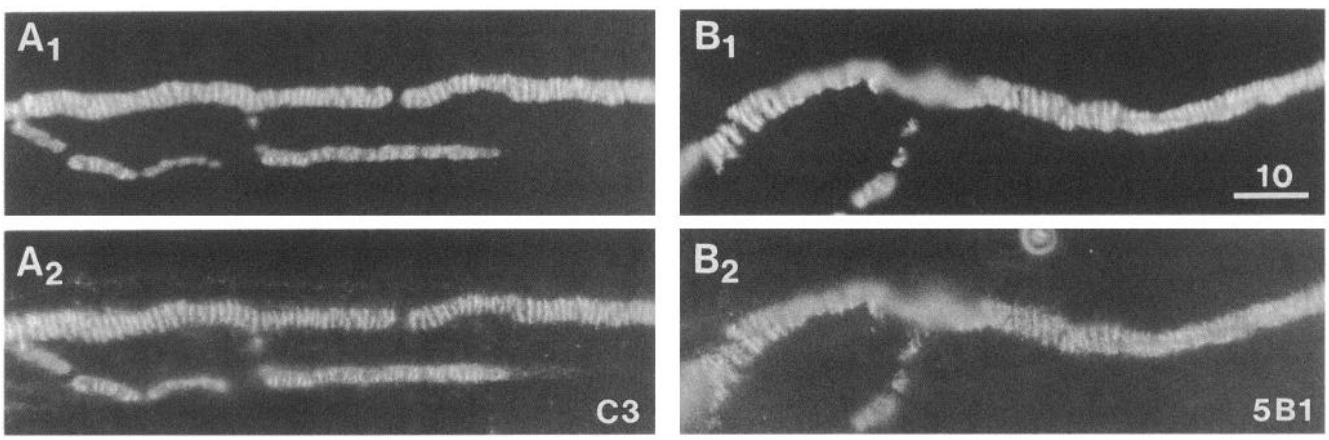

Figure 8. Immunofluorescence at synapses in adult *Rana* sartorius muscle. RαBT fluorescence is seen in A_1 and B_1. The corresponding immunofluorescence with C3 and with 5B1 is seen in A_2 and B_2, respectively. Note the characteristic banded pattern, indicating that antibody binding sites extended into the junctional folds. Some nonspecific immunofluorescence, associated with connective tissue, is also apparent in A_2. Scale bar, 10 μm.

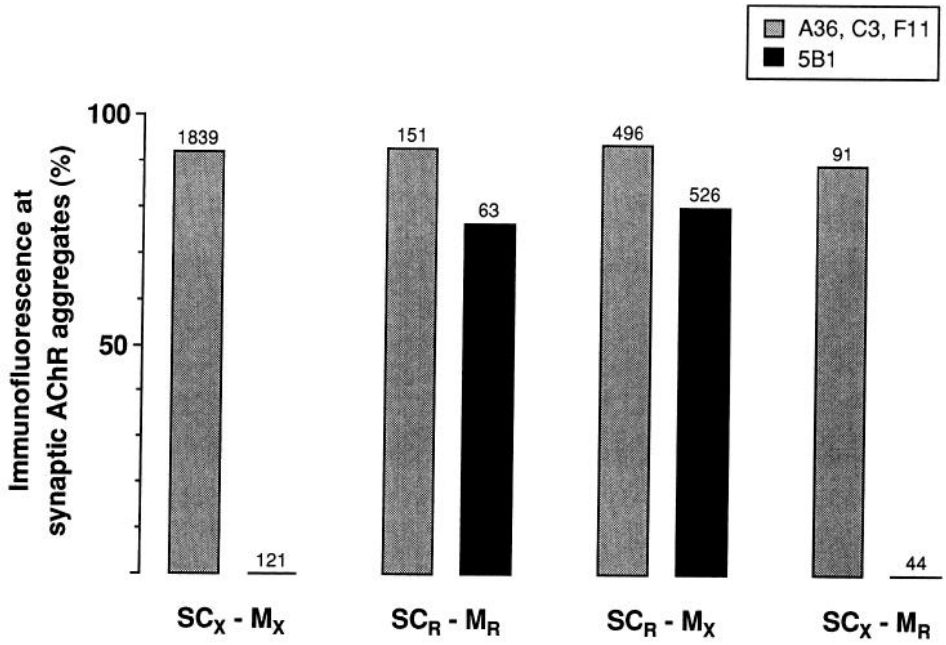

Figure 9. Incidence of colocalization of anti-agrin immunofluorescence at synaptic aggregates of AChRs in different combinations of coculture. For each coculture combination, values obtained with anti-36, C3, and F11 are plotted on the *left* (*shaded columns*) and values obtained with 5B1 are plotted on the *right* (*solid columns*). Note that 5B1 immunofluorescence was seen only in SC_R-M_R and SC_R-M_X cocultures. The *numbers* of AChR aggregates counted are indicated above the columns. The data for SC_X-M_X are from Figure 4.

immunofluorescence at synaptic AChR aggregates (Fig. 10). As was the case for SC_R-M_R cultures, the incidence of colocalization of anti-agrin immunofluorescence at synaptic AChR aggregates was a little less for 5B1 than for anti-36, C3, and F11 (Fig. 9). Since 5B1 is reactive in *Rana* but not in *Xenopus,* the agrin-like molecules detected by 5B1 at SC_R-M_X contacts must have been supplied by the SC_R neurons.

In SC_X-M_R cultures, anti-36 and C3 immunofluorescence (F11 was not tested) was preferentially localized at synaptic aggregates of AChRs and the incidence of colocalization was similar to that obtained for the other coculture combinations (Fig. 9). On the other hand, there was no detectable 5B1 immunofluorescence along the SC_X-M_R contacts (Figs. 9, 11). This means that few if any agrin-like molecules recognized by 5B1 were supplied by M_R cells to these synapses. The simplest explanation to account for the anti-36 and C3 immunofluorescence at SC_X-M_R contacts is that *Xenopus* neurons, like *Rana* neurons, supply agrin-like molecules to the synapses they form on muscle cells.

Discussion

Considerable support has accumulated for the hypothesis that agrin, or a closely related molecule, is the primary neuronal agent involved in triggering the aggregation of AChRs in the postsynaptic membrane during neuromuscular synaptogenesis (McMahan and Wallace, 1989; Wallace, 1991). The evidence includes the presence of agrin-like molecules in the cell bodies of embryonic motor neurons from the onset of neuromuscular synaptogenesis (Magill-Solc and McMahan, 1988) and their anterograde transport along axons (Magill-Solc and McMahan, 1989). According to the hypothesis, agrin molecules are externalized by growing axons, and as a result of binding to their receptors on muscle cells, they trigger the formation of postsynaptic specializations including a high density of AChRs. The externalized agrin becomes associated with the nascent synaptic basal lamina.

The present study constitutes the first demonstration that

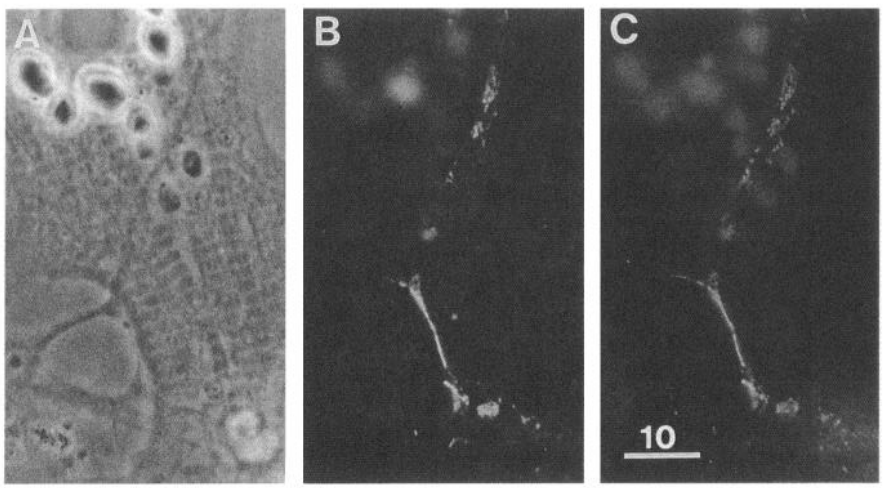

Figure 10. 5B1 immunofluorescence in an SC_R-M_X culture. Phase contrast (*A*), RαBT fluorescence (*B*), and immunofluorescence (*C*) are shown for the same field. Immunofluorescence was colocalized with the AChR aggregates along the nerve–muscle contacts. Scale bar, 10 μm.

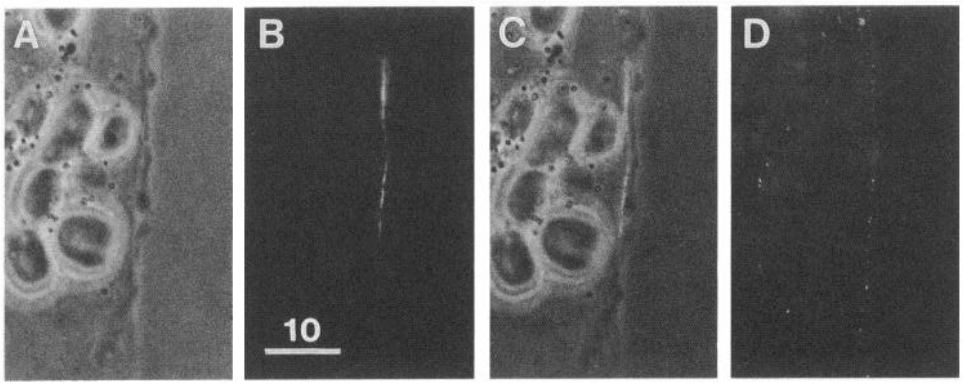

Figure 11. Lack of 5B1 immunofluorescence in an SC_X-M_R culture. *A*, Phase contrast, showing an SC_X neurite coursing along the edge of an M_R cell. Small phase-dark particles, which may be pigment granules, were commonly seen in the M_R cells. *B*, RαBT fluorescence. *C*, Combined phase contrast and RαBT fluorescence, showing fluorescence at the boundary between the neurite and muscle cell. *D*, Immunofluorescence. Scale bar, 10 μm.

neurons do indeed supply agrin-like molecules to embryonic nerve–muscle synapses. The evidence is most direct for *Rana* neurons and also indicates that the molecules recognized by the anti-agrin antibody 5B1 are not supplied to the synapse by *Rana* muscle cells. The evidence, though less direct, suggests that *Xenopus* neurons also supply agrin-like molecules to the synapses they form with muscle. Agrin-like molecules were concentrated at nerve-induced synaptic aggregates of AChRs but were virtually absent elsewhere on muscle cells, even at well-developed nonsynaptic aggregates of AChRs that form in the absence of innervation. Agrin-like molecules were also associated with growing neurites and with the earliest-detectable, nerve-induced microaggregates of AChRs along nerve–muscle contacts less than 2 hr old. Altogether, our findings strongly support the conclusion that neuronally derived agrin-like molecules are present at newly forming synaptic sites from the onset of nerve-induced aggregation of AChRs.

Anti-agrin immunofluorescence was not detected at about 10% of the AChR aggregates along nerve–muscle contacts. There are several possible explanations for this result, none of which undermine the above conclusions. It may be that the antibodies failed to reach their binding sites because of restricted access (see Materials and Methods), that the AChR aggregates in question were nonsynaptic and were contacted by the neurite simply by chance, or that they were nerve induced and originally did have detectable quantities of agrin-like molecules associated with them but the neurites stopped resupplying the molecules to these sites. Another possible explanation for the apparent lack of agrin-like molecules at a small percentage of the AChR aggregates along nerve–muscle contacts bears on the mechanism of action of agrin. It has been estimated that when agrin is applied diffusely to embryonic chick muscle cells by adding it to their culture medium, a single molecule of agrin may be able to cause some 160 AChRs to aggregate (Nitkin et al., 1987). Perhaps in the present study there were sufficient quantities of neuronally derived agrin even at those synaptic AChR aggregates where anti-agrin immunofluorescence was not detected.

The estimated potency of a single agrin molecule has led to the notion that the binding of agrin to its receptor triggers an intracellular cascade in the muscle cell (Nitkin et al., 1987; McMahan and Wallace, 1989). Current evidence suggests that an early step in this cascade is the phosphorylation of the β-subunit of the AChR by a tyrosine kinase (Wallace, 1991; Wallace et al., 1991). The molar ratio of agrin to AChRs at nerve-induced aggregates of AChRs is unknown. Assuming a ratio of 1:160 and an AChR density of 10,000/μm^2, microaggregates 0.3 μm in diameter (see Figs. 5*D*, 6) would contain about 700 AChRs and four or five agrin molecules. Presumably, so few agrin molecules would not be detected by standard immunofluorescence techniques. Since the immunofluorescence at microaggregates of AChRs was often more intense than the RαBT fluorescence, it may be that the molar ratio at the earliest-forming synaptic aggregates of AChRs is much higher than 1:160. Perhaps agrin-like molecules can influence AChR distribution on muscle cells by more than one mechanism and their concentration at highly localized sites ensures that aggregation of AChRs is limited to those specific sites.

Recent evidence indicates that agrin is a member of a family of molecules and that only agrin, but not closely related isoforms, can induce AChR aggregation (Ruegg et al., 1991). This raises the question whether the immunofluorescence we observed was due to more than one member of the agrin family and whether the closely related, inactive isoforms predominated over agrin at synaptic sites and along growing neurites. At present, it is not known if individual neurons express more than one of the agrin proteins; a recent report indicates that motor neurons in the chick embryo express primarily active agrin (Tsim et al., 1991). In addition, the antibodies we used bound to AChR-aggregating molecules—probably agrin—from *Xenopus* brain. Thus, it is likely that the neuronally derived molecules visualized in the present study were predominantly active agrin.

The presence of agrin-like molecules on the surface of growing neurites is in line with the prediction (Rupp et al., 1991) that agrin can bind to motor neurons. Appropriately transfected COS or CHO cells also exhibit agrin on their surface (Campanelli et al., 1991). Our finding raises the possibility that agrin-like molecules normally interact with their "receptors" on embryonic muscle cells while still bound to the surface of the neurite. In embryonic chick muscle cells in culture, putative receptors for *Torpedo* agrin appear to be distinct from AChRs (Nastuk et al., 1991). On the other hand, the precision of colocalization of anti-agrin immunofluorescence at microaggregates of AChRs (Figs. 5*D*, 6) suggests that AChRs or closely associated molecules may also be receptors for agrin-like proteins (see also Hartman et al., 1991). If this notion is correct, then agrin-like molecules on the surface of growing neurites could act as a trap for AChRs, and this interaction would be the initial event in the development of the postsynaptic membrane. Whether or not this is the case, it seems likely that the microaggregates of agrin-like molecules along early nerve–muscle contacts represent the primary sites of nerve-induced clustering of AChRs.

Nonsynaptic regions of muscle cells did not exhibit anti-agrin immunofluorescence, nor did we obtain evidence for a contribution by muscle cells to the agrin-like molecules at synapses,

yet other studies, employing chick and rat, have indicated that agrin-like molecules are expressed by muscle cells (Fallon and Gelfman, 1989; Rupp et al., 1991). In the case of chick, the evidence also indicates that muscle cells and other non-neuronal cells express agrin-related proteins that differ in function and structure from agrin in motor neurons (Godfrey, 1991; Ruegg et al., 1991). Perhaps muscle-derived agrin-like molecules were present at synaptic and nonsynaptic AChR aggregates in our study but the antibodies we used were not reactive with the agrin-like isoforms expressed by frog muscle cells. In support of this suggestion, we have recently found an anti-agrin antibody that does reveal immunofluorescence at nonsynaptic AChR aggregates on embryonic frog muscle cells in culture (M. W. Cohen and E. W. Godfrey, unpublished observations).

References

Anderson MJ, Cohen MW (1977) Nerve-induced and spontaneous redistribution of acetylcholine receptors on cultured muscle cells. J Physiol (Lond) 268:757–773.

Anderson MJ, Cohen MW, Zorychta E (1977) Effects of innervation on the distribution of acetylcholine receptors on cultured amphibian muscle cells. J Physiol (Lond) 268:731–756.

Bornstein MB (1958) Reconstituted rat-tail collagen used as substrate for tissue cultures on coverslips in Maximow slides and roller tubes. Lab Invest 7:134–137.

Campanelli JT, Hoch W, Rupp F, Kreiner T, Scheller RH (1991) Agrin mediates cell contact-induced acetylcholine receptor clustering. Cell 67:909–916.

Chow I, Cohen MW (1983) Developmental changes in the distribution of acetylcholine receptors in the myotomes of *Xenopus laevis*. J Physiol (Lond) 339:553–571.

Cohen MW (1972) The development of neuromuscular connections in the presence of *d*-tubocurarine. Brain Res 41:457–463.

Cohen MW, Godfrey EW (1991) Neuronally derived agrin-like molecules appear early at embryonic frog nerve-muscle synapses in culture. Soc Neurosci Abstr 17:179.

Cohen MW, Anderson MJ, Zorychta E, Weldon PR (1979) Accumulation of acetylcholine receptors at nerve-muscle contacts in culture. Prog Brain Res 49:335–349.

Cohen MW, Rodriguez-Marin E, Wilson EM (1987) Distribution of synaptic specializations along isolated motor units in *Xenopus* nerve-muscle cultures. J Neurosci 7:2849–2861.

Fallon JR, Gelfman CE (1989) Agrin-related molecules are concentrated at acetylcholine receptor clusters in normal and aneural developing muscle. J Cell Biol 108:1527–1535.

Fallon JR, Nitkin RM, Reist NE, Wallace BG, McMahan UJ (1985) Acetylcholine receptor-aggregating factor is similar to molecules concentrated at neuromuscular junctions. Nature 315:571–574.

Frank E, Fischbach GD (1979) Early events in neuromuscular junction formation *in vitro*. Induction of acetylcholine receptor clusters in the postsynaptic membrane and morphology of newly formed synapses. J Cell Biol 83:143–158.

Godfrey EW (1991) Comparison of agrin-like proteins from the extracellular matrix of chicken kidney and muscle with neural agrin, a synapse organizing protein. Exp Cell Res 195:99–109.

Godfrey EW, Nitkin RM, Wallace BG, Rubin LL, McMahan UJ (1984) Components of *Torpedo* electric organ and muscle that cause aggregation of acetylcholine receptors on cultured muscle cells. J Cell Biol 99:615–627.

Godfrey EW, Dietz ME, Morstad AL, Wallskog PA, Yorde DE (1988a) Acetylcholine receptor-aggregating proteins are associated with the extracellular matrix of many tissues in *Torpedo*. J Cell Biol 106:1263–1272.

Godfrey EW, Siebenlist RE, Wallskog PA, Walters LM, Bolender DL, Yorde DE (1988b) Basal lamina components are concentrated in premuscle masses and at early acetylcholine receptor clusters in chick embryo hindlimb muscles. Dev Biol 130:471–486.

Goldfarb J, Cantin C, Cohen MW (1990) Intracellular and surface acetylcholine receptors during the normal development of a frog skeletal muscle. J Neurosci 10:500–507.

Hartman DS, Millar NS, Claudio T (1991) Extracellular synaptic factors induce clustering of acetylcholine receptors stably expressed in fibroblasts. J Cell Biol 115:165–177.

Hirano Y, Kidokoro Y (1989) Heparin and heparan sulfate partially inhibit induction of acetylcholine receptor accumulation by nerve in *Xenopus* culture. J Neurosci 9:1555–1561.

Kidokoro Y, Anderson MJ, Gruener R (1980) Changes in synaptic potential properties during acetylcholine receptor accumulation and neuro-specific interactions in *Xenopus* nerve-muscle cell culture. Dev Biol 78:464–483.

Kullberg RW, Lentz TL, Cohen MW (1977) Development of the myotomal neuromuscular junction in *Xenopus laevis*: an electrophysiological and fine-structural study. Dev Biol 60:101–129.

Magill-Solc C, McMahan UJ (1988) Motor neurons contain agrin-like molecules. J Cell Biol 107:1825–1833.

Magill-Solc C, McMahan UJ (1989) Agrin-like molecules in motor neurons. J Physiol (Paris) 83:18–21.

McMahan UJ, Wallace BG (1989) Molecules in basal lamina that direct formation of synaptic specializations at neuromuscular junctions. Dev Neurosci 11:227–247.

Nastuk MA, Lieth E, Ma J, Cardasis CA, Moynihan EB, McKechnie BA, Fallon JR (1991) The putative agrin receptor binds ligand in a calcium-dependent manner and aggregates during agrin-induced acetylcholine receptor clustering. Neuron 7:807–818.

Nieuwkoop PD, Faber J (1967) Normal table of *Xenopus laevis* (Daudin), 2d ed. Amsterdam: North Holland.

Nitkin RM, Smith MA, Magill C, Fallon JR, Yao MY-M, Wallace BG, McMahan UJ (1987) Identification of agrin, a synaptic organizing protein from *Torpedo* electric organ. J Cell Biol 105:2471–2478.

Reist NE, Magill C, McMahan UJ (1987) Agrin-like molecules at synaptic sites in normal, denervated, and damaged skeletal muscles. J Cell Biol 105:2457–2469.

Ruegg MA, Tsim KWK, Horton SE, Kröger S, McMahan UJ (1991) Agrin is a member of a group of molecules having high structural similarity but differing in function. Soc Neurosci Abstr 17:178.

Rupp F, Payan DG, Magill-Solc C, Cowan DM, Scheller RH (1991) Structure and expression of a rat agrin. Neuron 6:811–823.

Shumway W (1940) Stages in the normal development of *Rana pipiens*. Anat Rec 78:139–144.

Swenarchuk LE, Champaneria S, Anderson MJ (1990) Induction of a specialized muscle basal lamina at chimaeric synapses in culture. Development 110:51–61.

Tsim KWK, Ruegg MA, Escher G, Kröger S, McMahan UJ (1991) cDNA that encodes agrin. Soc Neurosci Abstr 17:178.

Wallace BG (1990) Inhibition of agrin-induced acetylcholine-receptor aggregation by heparin, heparan sulfate, and other polyanions. J Neurosci 10:3576–3582.

Wallace BG (1991) The mechanism of agrin-induced acetylcholine receptor aggregation. Philos Trans R Soc Lond [Biol] 331:273–280.

Wallace BG, Qu Z, Huganir RL (1991) Agrin induces phosphorylation of the nicotinic acetylcholine receptor. Neuron 6:869–878.